Classical and quantum dynamics of electrons in open equilateral triangular billiards

L. Christensson, H. Linke, and P. Omling
Solid State Physics, Lund University, Box 118, S-221 00 Lund, Sweden

P. E. Lindelof
Niels Bohr Institute, University of Copenhagen, Universitetsparken 5, DK-2100 Copenhagen Ø, Denmark

I. V. Zozoulenko, and K.-F. Berggren
Theoretical Physics Group, Department of Physics and Measurement Technology, Linköping University, S-581 83 Linköping, Sweden
(Received 27 August 1997)

Experimental and theoretical studies of the electron dynamics in open equilateral triangular billiards are presented. We focus on the question to what extent classical mechanics can be used to model electron transport in comparison to a fully quantum-mechanical treatment. The classical simulations of the magnetoresistance, which are based on a billiard-ball model, agree in great detail with the temperature averaged, gross features of the measured data. The frequency of experimentally observed conductance fluctuations can be related to a simple closed electron orbit, which, in turn, is shown to be particularly important for classical electron dynamics. The magnetoresistance calculated quantum mechanically shows, in addition to the (classical) gross features, also quasiperiodic conductance fluctuations in the same frequency range as experimentally observed. We address the effect of the distortion of the classical trajectories induced by the magnetic field on the frequency of the conductance fluctuations. This effect appears to be less important in small samples. In order to also visually compare the classical and quantum-mechanical pictures of electron transport, plots of the particle density inside the billiard are presented, which were obtained with both classical and quantum-mechanical methods. The resemblance is weak at low-magnetic fields, while at high fields strikingly similar images are obtained with the two techniques. [S0163-1829(98)08519-1]

I. INTRODUCTION

Two-dimensional cavities of arbitrary shape can be fabricated from semiconductor heterostructures such as $GaAs/Al_xGa_{1-x}As$.[1] For high-quality samples, the typical size can be smaller that the mean-free path for both elastic and inelastic scattering at low temperatures, but larger than the Fermi wavelength of the electrons. Transport through such cavities, called billiards, is then ballistic, phase coherent, and sensitive to the shape of the boundaries at which the electrons are reflected.[2,3] The transport properties of electron billiards provide an experimental and controllable tool for the investigation of the type of dynamics obeyed by the electrons inside the cavity. Depending on the geometric shape and how electrons are injected into the billiard, the classical motion will be regular or chaotic. At the same time the size will determine whether the dynamics is wave mechanical or classical, or as here, in the border area between classical and quantum behavior. Hence, we will focus on the case of an equilateral triangle subject to a homogeneous perpendicular magnetic field. The classical motion of an electron bouncing from wall to wall inside such a cavity is regular in the absence of a field. The corresponding quantum states are also available in analytic form[4-7] and the level statistics for nearest-level separations shows an abundance of level crossings, as expected for a regular system. For a finite magnetic field the classical motion becomes irregular and quantum levels start to repel each other.

Transport through a large triangular electron billiard in a perpendicular magnetic field and with two opposite leads has been investigated recently.[8] By comparing the measured magnetoresistance with simulations of classical electron trajectories the positions of the resistance peaks could be correlated with specific commensurate trajectories. Also the overall gross features of the classically simulated data were found to be in good agreement with measured data. These previous studies were concerned with the experimental regime where thermal broadening and inelastic scattering are effective such that quantum interference effects are suppressed. In the present work, we focus on the fine structure that emerges in the form of conductance fluctuations when the temperature is lowered, and we will present results from fully quantum-mechanical calculations as well as complementary classical simulations. In a detailed comparison of the two approaches we will discuss a number of fundamental questions. The first one deals with the usefulness of (semi)classical dynamics to model transport in a regime where quantum interference effects are observed. For a large dot like ours, one is, in practice, close to the regime in which electrons should behave as classical objects. If this is the case, classical modeling is a convenient and correct alternative to more cumbersome quantum-mechanical approaches. Interference effects due to the wave mechanical nature of the electrons then enter only as corrections to a basically classical picture. The second question is therefore how to explain the conductance fluctuations caused by electron interference. We will discuss the origin of the fluctuations in terms of periodic orbits and full quantum-mechanical solutions, and compare the results. The third question is to which extent the classical electron orbits, on which a semiclassical interpretation of the magnetoresistance is based, are reflected by the quantum-mechanical wave functions. We will therefore com-

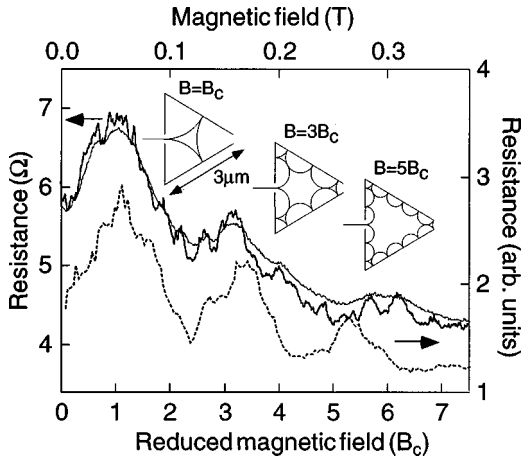

FIG. 1. Measured magnetoresistance of an equilateral triangular electron billiard at 4.4 K (thin solid curve) and 0.3 K (thick solid curve). Indicated are the trajectories of electrons that enter the billiard along the symmetry axis through the side opening at $B/B_c=1,3,5$, respectively (see text), which are thought to be related to the local maxima of the resistance. Dashed curve: magnetoresistance (in arbitrary units) as obtained from simulations of classical electron orbits (from Ref. 8). Apart from the fast fluctuations that are due to statistical noise, the simulations show extensive similarity with the experimental data recorded at $T=4.4$ K.

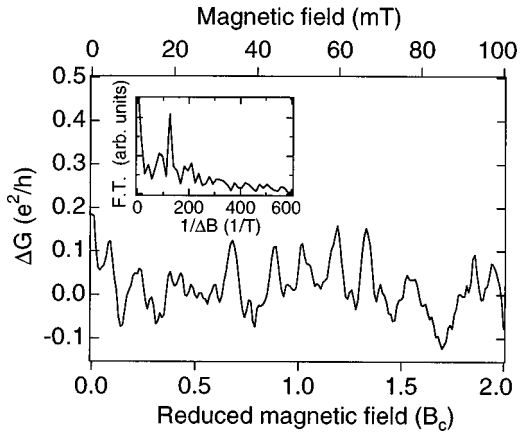

FIG. 2. The plot shows the conductance fluctuations $\Delta G=[G(T=0.3\ \mathrm{K})-G(T=4.4\ \mathrm{K})]$. In the region of the maximum of the resistance around $B=B_c\simeq 50$ mT, the fluctuations are quasiperiodic and the amplitude is enhanced. The inset shows the Fourier transform of the data in the range $0<B<1.5B_c$.

pare classical and quantum-mechanical electron-density distributions at a number of different magnetic fields.

Our paper is organized as follows. In Sec. II we give a brief presentation of the measurements and introduce the classical ball trajectories associated with the resistance maxima. In order to make our presentation more comprehensive, we also summarize some previous results. In Sec. III we discuss the theoretical modeling of magnetotransport. After some general comments we present results of classical simulations in Sec. III A and from full wave-mechanical considerations in Sec. III B, where we also compare the two approaches. The results of our discussions are finally summarized in Sec. IV.

II. EXPERIMENTS

The experimental data presented in this work, which are representative of data from several different devices that were studied, were obtained from a wet-etched $GaAs/Al_xGa_{1-x}As$ electron billiard with the lithographic shape of an equilateral triangle of side 3 μm. The Fermi energy of the unpatterned two-dimensional electron gas was $E_F=10$ meV and the mean free path was 10 μm. The point contacts at the center of one side and at one tip (inset of Fig. 1) had an estimated electric width of 100 nm and the number of subbands in the channels was about three (Fermi wavelength $\lambda_F=45$ nm). Further details about the device have been reported elsewhere.[8] All resistance measurements were carried out in a four-terminal geometry using a current-controlled lock-in technique with an excitation voltage of less that 10 μV.

The thin solid curve in Fig. 1 is the magnetoresistance of the device at the temperature $T=4.4$ K. It has been found that at this relatively high temperature, at which quantum interference effects are absent, the magnetoresistance data can be explained in great detail by commensurability effects due to the classically ballistic motion of the electrons inside the triangular billiard.[8] In particular, the three maxima of the magnetoresistance can be related to reflected electron trajectories present when the magnetic field is an odd multiple of a characteristic field B_c, as indicated in Fig. 1. Here B_c is defined as the magnetic field when the cyclotron radius $l_c=mv_F/eB$ equals half the length of the side of the triangle, where v_F is the Fermi velocity and m is the effective mass of the electron. The reason for the importance of these particular trajectories was found to be their relative stability towards small changes of initial conditions, and their relatively small length.[8] When the temperature is decreased below a few kelvin, such that phase destructive electron-electron interactions[1,9] and thermal averaging are sufficiently suppressed, quantum interference effects manifest themselves as reproducible fluctuations of the magnetoresistance (thick solid curve in Fig. 1). These fluctuations are thought to be due to the interference of electrons inside the billiard.[2,3,10-12]

In the following we focus attention on the fluctuations in the magnetic-field region around the global maximum of the magnetoresistance at $B=B_c\simeq 50$ mT. In Fig. 2, the difference between the data obtained at 0.3 K and at 4.5 K is shown, plotted as the change of the conductance ΔG. The rms amplitude of the conductance fluctuations is about $0.06e^2/h$. A Fourier transform of these data in the range between zero and $1.5B_c$ (inset of Fig. 2) shows a dominant frequency $f\simeq 130\ \mathrm{T}^{-1}$, which corresponds to an area of $f/(e/h)=0.54\ \mu\mathrm{m}^2$. Recently, periodic conductance fluctuations in electron billiards have been related to particular classical electron trajectories[3,13-15] (see also Refs. 6, 16, and 17 for classical periodic orbits and scarring). In our case, the dominant frequency is found only in the magnetic-field range around the maximum at $B=B_c$. Therefore, we suggest that the periodic fluctuations are related to the reflected trajectory thought to be the reason for the resistance maximum at $B=B_c$ (Fig. 1). The area (A) enclosed by this trajectory equals $0.040a^2$, where a is the electric side length of the triangle. From the position of the peak at $B=B_c$ we find $a=3.6$ μm, which gives $A=0.52\ \mu\mathrm{m}^2$, in strikingly good agreement with the observed frequency and with previous estimates of

the size of the triangle.[8] We note, however, that our estimates may be subject to uncertainties related to, for instance, the correct assignment of the electron density inside the billiard, the location of B_c, and the true nature of the confining walls. We will return to the periodic fluctuations in connection with the full quantum-mechanical modeling.

III. THEORY

The quantity directly measured in the experiment is the resistance of the cavity, the inverse of which gives the conductance G. The two-probe conductance is in turn given by the Landauer-Büttiker formula (see, for example, Ref. 1)

$$G=\frac{2e^2}{h}T_{i,j}, \tag{1}$$

where $T_{i,j}$ is the total transmission for electrons being injected from lead j and subsequently collected in lead i, where $i\neq j$ refer to the different leads 1 and 2, i.e., we have either $T_{1,2}$ or $T_{2,1}$, depending on the direction of the current.

In the following sections we will determine the transmission of a triangular billiard from, first, simulations in which electrons are treated as classical charged particles and, second, from a full quantum-mechanical calculation. In the classical case, the transmission is obtained from the distribution of trajectories for particles injected at different angles from one of the leads. The total reflection $R_{j,j}$ is related to $T_{i,j}$ by the conservation of particles. If N is the number of available channels in the leads, one has $T_{i,j}+R_{j,j}=N$. In the discussion of the classical case we will assume a scale in which $T_{i,j}+R_{j,j}=1$, such that $T_{i,j}$ is simply the probability that a classical particle is transmitted through the billiard.

In the quantum-mechanical case the conductance at zero temperature is related to the complex transmission matrix $\mathbf{t}$ as

$$G(E_F)=\frac{2e^2}{h}\mathrm{Tr}(\mathbf{t}\mathbf{t}^{\dagger}), \tag{2}$$

where $t_{\alpha,\beta}=(\mathbf{t})_{\alpha,\beta}$ is the transmission amplitude from incoming mode β in one lead into mode α in the other, collecting lead. The relation to the total transmission $T_{i,j}$ is then

$$T_{i,j}=\sum_{\alpha\in i,\beta\in j}|t_{\alpha,\beta}|^2. \tag{3}$$

It follows that $T_{i,j}+R_{j,j}=N$. With these preliminaries we will now discuss the classical and quantum cases separately.

A. Simulations using classical trajectories

The result of a classical simulation of the magnetoresistance is shown in Fig. 1. In the simulation, electrons that start at Fermi velocity at different initial angles from the opening in the side (named 1) were traced inside the billiard until they escaped through openings 1 or 2. The ratio of the electrons transmitted through the billiard at each setting of the magnetic field, $T_{2,1}(B)$, was determined and then related to the resistance (R) by setting $R(B)\propto T_{2,1}(B)^{-1}$. The electrons were treated entirely as classical, charged particles in a hard-wall potential. A realistic amount of impurity scattering was taken into account by changing the direction of motion randomly after an exponentially distributed random distance of travel (for further details, see Linke *et al.*[8]). From a comparison of the measured and the simulated data in Fig. 1 it is apparent that the simulation reproduces the overall behavior of the experimental data, including some fine structures with the exception of the statistical noise. In particular, the positions of the major resistance maxima that can be related to the simple reflected electron trajectories indicated in Fig. 1 are reproduced in the simulation. Only the position of the maximum around $B/B_c=5$ appears to be somewhat shifted towards lower fields relative to the measured value.

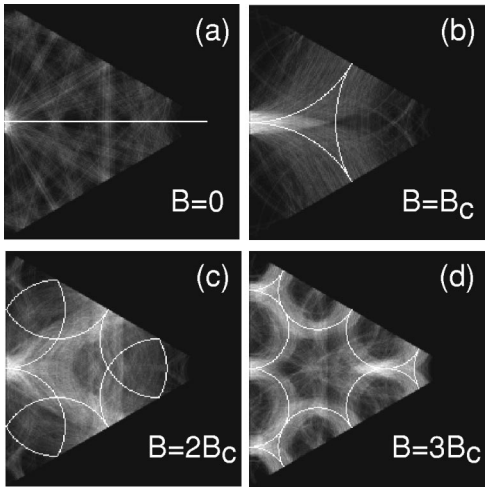

FIG. 3. Superpositions of the trajectories of 5000 electrons injected through the side opening at the magnetic fields indicated. Only the trajectories of electrons reflected by the billiard are plotted. The white lines are the trajectories of electrons injected along the symmetry axis. At $B=0$ these electrons are transmitted. At $B/B_c=1$ and $B/B_c=3$, where many electrons follow orbits similar to the ones indicated, the probability of reflection is high and the magnetoresistance reaches a maximum. The reflecting trajectory at $B=2B_c$ is unstable and only few electrons follow this or similar trajectories; no maximum of the resistance is observed at this value of the magnetic field.

The semiclassical interpretation of the magnetoresistance given in Sec. II and in Ref. 8 emphasizes a small number of specific electron trajectories (Fig. 1). In a more complete description, the magnetoresistance and the conductance fluctuations should be viewed as the result of a superposition of all possible electron trajectories inside the billiard. In order to visualize this situation, we have simulated a large number of electron trajectories with different initial conditions. In an approach similar to that described above, the classical trajectories of over 5000 electrons, starting at the Fermi velocity from one contact opening, were traced inside the billiard until the electrons escaped. The initial angle was cosine distributed between $\pm 90°$ and the starting point was evenly distributed within the opening. No impurity scattering or electron-electron interaction was taken into account. The longest electron trajectories, about 10% of the total number, were neglected. This was done because long trajectories make a disproportionally large contribution to the classical density of trajectories, while they are in reality unimportant because they are randomized by impurity scattering.

Figure 3 shows a superposition of the trajectories of all electrons entering and leaving the billiard through the side

opening. Trajectories of transmitted electrons are not included. This plot can be viewed as the classical particle-density distribution of the *reflected* electrons. Figures 3(a)–3(d) are for $B/B_c=0,\ 1,\ 2$, and 3, respectively. The white lines are the ideal trajectories of electrons injected along the symmetry axis of the triangle. At $B=0$, electrons injected in the forward direction are transmitted, in agreement with the resistance minimum observed at this field. At $B/B_c=1$ and at $B/B_c=3$, a significant number of electrons follows reflected trajectories, which are similar to the white lines, supporting the interpretation of the peaks in the magnetoresistance (Fig. 1). In contrast, at $B/B_c=2$, where no maximum of the resistance is observed, the white line is not a representative electron trajectory. Instead the particle density is smeared out over a large portion of the area of the triangle, and no simple trajectories can be found. The reason is that the Lyapunov exponent averaged over all injection angles at $B/B_c=2$ is relatively large, and the white trajectory in Fig. 3(c) is comparably unstable.[8]

Also, the semiclassical interpretation of the Aharanov-Bohm-like periodic conductance fluctuations experimentally observed at about $B\simeq B_c$ (Fig. 2) is supported by Fig. 3. The fluctuation frequency was found to correspond to the area enclosed by the trajectory of electrons injected through the base contact along the symmetry axis at $B=B_c$. In fact, a significant number of the reflected electrons follows trajectories that enclose approximately the same area [Fig. 3(b)]. Also, at $B=0$, a fraction of the electrons injected follows a similar trajectory, but not at the higher fields. This finding is in agreement with our quantum-mechanical calculations of the transmission that predict quasiperiodic oscillations of this frequency at $B\lesssim B_c$.

So far in the discussion of the classical electron trajectories we have considered exclusively reflected electron orbits that start from the side opening. The success of this selective model may appear surprising because one could expect that all possible trajectories, including transmitted ones, need to be considered for a complete understanding. However, as we will show in the following, the classical magnetoresistance of a general two-terminal billiard is entirely described by considering either only transmitted or only reflected electron trajectories starting from only one of the openings. This is due to two factors: First, because of time reversal symmetry, any arbitary electron trajectory that connects the two leads can be followed in either direction, provided that the magnetic field is reversed simultaneously with the electron motion. Therefore, equally many classical initial conditions lead to the transmission of electrons starting at either of the two contacts, and the probabilities for transmission are equal, $T_{i,j}(+B)=T_{j,i}(-B)$. Second, the probabilities for reflection are related to the probabilities for transmission by $R_{i,i}=(1-T_{j,i})$, and therefore,

$$[1-R_{1,1}(+B)]=T_{2,1}(+B)=T_{1,2}(-B)=[1-R_{2,2}(-B)]. \tag{4}$$

Consequently, one of the four parameters contains the information on the other three. However, it should be noted that only the transmitting trajectories are the same for either direction of the current, while the reflecting trajectories are topographically different if the billiard does not have a symmetry axis perpendicular to the direction of the current. This is illustrated in Fig. 4 in which (a) and (b) show superpositions of transmitted electron orbits at $B/B_c=3$, starting at either opening. In fact, the resulting particle density plots are strikingly similar. In contrast, the corresponding plots of reflected electron trajectories do not show similarities because our triangular billiard lacks a symmetry axis perpendicular to the current direction [(c) and (d) in Fig. 4].

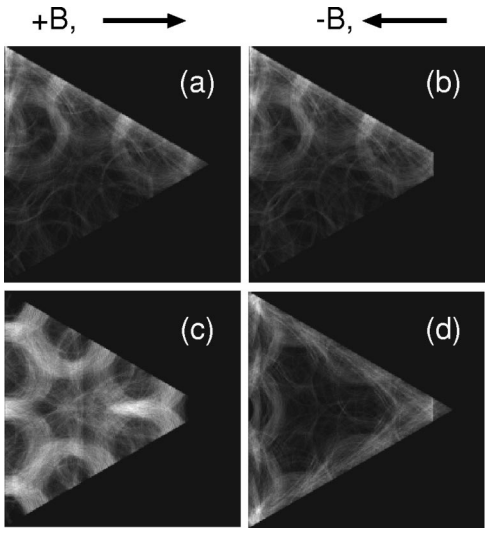

FIG. 4. Superpositions of electron trajectories, starting at $B=+3B_c$ from the side opening [(a) and (c)], and from the tip opening at $B=-3B_c$ [(b) and (d)], respectively. The arrows indicate the direction of injection. The upper two figures show the transmitted orbits only, while the lower show the reflected orbits. Because of time-reversal symmetry, the transmitting trajectories are identical in the two cases, while the reflected orbits are different.

Although the above discussion shows that it is formally sufficient to consider only the reflected trajectories starting from the side contact, it remains puzzling that we were not able to find a similarly descriptive explanation for the magnetoresistance when considering any of the other three sets of trajectories.

B. Wave-mechanical picture

The basic picture of electrons injected into classical trajectories in the triangular cavity is evidently a strong one. An attractive aspect is that the underlying physics becomes very transparent and easy to handle, conceptually as well as computationally. Gross features, such as the location of the major maxima and minima in the magnetoresistance, are predicted with considerable success. The reason is that the cavity is so large that the wave nature of the electrons appears to be of less importance. Hence, arguments based on classical particle dynamics and ''ray optics'' are valid. On the other hand, the observation of conductance fluctuations in the low-temperature magnetoresistance (Fig. 2) shows that the wave-mechanical nature of the electrons cannot be ignored altogether. We may say that we are in the border area between quantum mechanics and the classical world.

To gain an insight into how quantum and classical mechanics meet in our particular problem we have supplemented the classical simulations with a fully quantum-mechanical evaluation of the magnetotransport. In the

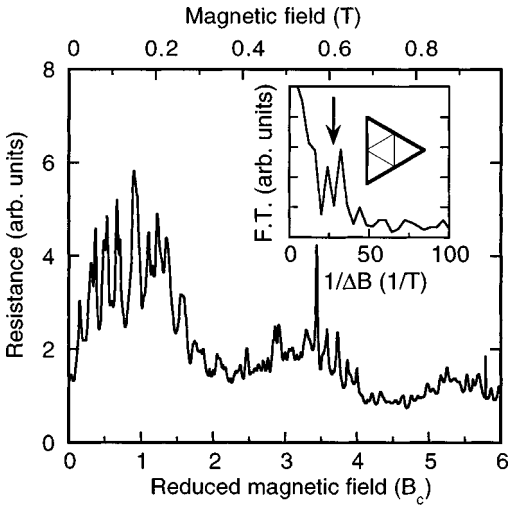

FIG. 5. Quantum-mechanical magnetoresistance (in arbitrary units) as obtained from the Green's-function calculations for an open, equilateral triangle with hard walls. The side of the triangle is 1 μm and the width of the two (infinitely long) leads is 0.1 μm. With the electron density $n_s=2.5\times10^{15}$ m^{-2} ($E_F=9$ meV) there are three open channels. The inset shows the Fourier transform (F.T.) of the data in the main figure in the range $0<B<1.5B_c$. Prior to the Fourier transformation the data were inverted such that the magnetoconductance was obtained. The arrow indicates the periodicity related to an undistorted electron orbit (semiclassical periodic orbit theory).

quantum-mechanical case the motion in the leads is quantized. The number of open modes or channels (occupied transverse states in the leads) depends on the dimensions of the leads, the magnetic field applied, and the position of the Fermi energy. To evaluate the conductance we have used the Landauer-Büttiker formalism, which relates the magnetoconductance of the device to its scattering characteristics as outlined above.

We have calculated the transmission matrix **t** on the basis of a hybrid, recursive Green's-function technique, which has proved to be numerically efficient for calculating quantum transport in large open cavities.[18] To simulate inelastic scattering effects within the cavity we have included a weak, imaginary optical potential of the approximate form $\sim i\hbar/\tau$, where the chosen inelastic lifetime $\tau=30$ ps agreed in magnitude with experimental values recently published.[19-22] This results in a general smoothing of the calculated conductance G, in practice resembling closely the effects of thermal broadening at finite temperatures. The inclusion of lifetime broadening is also convenient from a calculational point of view because the number of data points required to make reliable plots of G is drastically reduced. (On the other hand, there is a price to be paid for this convenience. When introducing lifetime broadening in this simple phenomenological way one breaks the symmetry with respect to a reversal of the field. Here the lifetime broadening is chosen to be small, of the same order as the thermal broadening, and for this reason we may simply ignore this complication.)

Figure 5 shows the magnetoresistance obtained from the Green's-function approach for an open triangle with hard walls. For computational reasons we have chosen the side of the triangle smaller than the real device, i.e., 1 μm instead of 3.6 μm. The width of the two leads is chosen as 0.1 μm. With an electron density $n_s=2.5\times10^{15}$ m^{-2}, and correspondingly, $E_F\simeq9$ meV, this leaves three channels open. As above, the results are plotted against B_c to emphasize general qualitative features and to faciliate comparisons with measurements. In the present case, $B_c=0.166$ T, about three times larger than for the experimental case because of the difference in size between the experimental and theoretical samples. The overall features of the theoretical results are obviously in good agreement with the measurements. The maximum at about $B/B_c=5$ is in closer agreement with the classical simulation than with the measured results, which indicates that the geometry of the experimental sample may not be perfect.[8] The experimentally observed low-temperature fluctuations are now reproduced in a qualitative way and can be traced to wave-mechanical interference, or standing wave effects.

One may discuss the conductance fluctuations in the following, somewhat simplistic way by assuming that they are essentially related to the density of states or shell structure of the nominally isolated billiard. Using for the moment the convenient semiclassical theory for this purpose, one finds[6,23] that the first isolated orbit in an equilateral triangle in zero magnetic field, indicated in the inset of Fig. 5 [and which is also visible among the trajectories in Fig. 3(a)], gives rise to a modulation $\cos[\phi/(\hbar/e)]$ of the density of states. Here $\phi=BA$ is the magnetic flux through the area $A=\sqrt{3}a^2/16\simeq0.11a^2$ enclosed by the periodic triangular orbit, undistorted by the magnetic field. The position of the arrow in the inset of Fig. 5, in which the Fourier transformation of the calculated magnetoconductance (i.e., of the inverted resistance data) is displayed, derives from these arguments and is clearly in good agreement with a single dominant frequency. One rough way of looking at the oscillations is therefore the following one. They would occur simply because the perpendicular magnetic field induces a diamagnetic shift of the shells associated with the triangular isolated orbit (Fig. 5, inset). This would lead to a gradual magnetic depopulation of the shells and result in a periodic modulation of the density of states at the Fermi level and, hence, the conductance on increasing magnetic field. Although this is a qualitatively appealing picture, it appears that we are facing a quantitative problem when the numerical values of theoretical and experimental periodicities are compared. Our quantum-mechanical simulation as presented in Fig. 5 appears to favor undistorted trajectories, while the measurements are consistent with trajectories distorted by the magnetic field, as indicated in Fig. 1. This discrepancy appears to be an interesting one from a conceptual point of view. In the case of the experimental data in Sec. II the semiclassical periodic orbit theory is applied to a large cavity ($a=3.6$ μm). In the theoretical modeling the side of the triangle was chosen much smaller for computational convenience ($a=1$ μm). Undoubtedly the distorted orbit is intuitively more appealing on classical grounds. One may therefore ask the relevant question whether the size of the cavity matters. Does it have to be a certain size before semiclassical arguments apply? To answer this question, we performed a number of simulations for a ranging from ~0.5 to ~2 μm. The answer is not clearcut. In fact, it turns out to be quite difficult to formulate a strict and consistent picture. With some good will, however, we may argue that the distorted orbits emerge

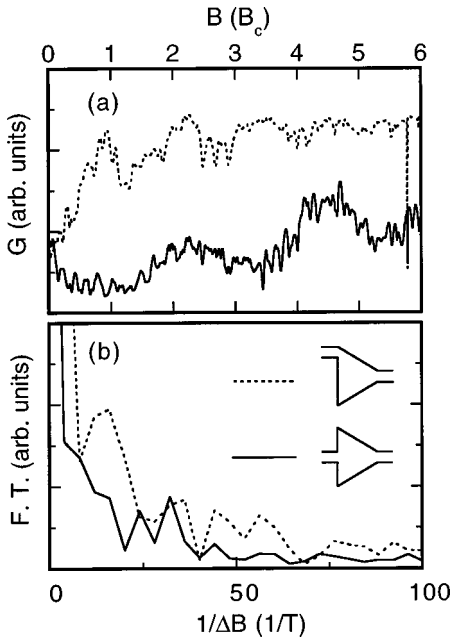

FIG. 6. (a) Quantum-mechanically calculated magnetoconductance and (b) the Fourier transformations for triangles with two different lead configurations, as indicated in the insets. The parameters used for the calculations are the same as were used for the data displayed in Fig. 5. The solid lines refer to the symmetric triangle, while the dashed lines refer to the unsymmetric structure. The contributing frequencies are the same in both cases, while their relative strength is different. This illustrates the importance of the lead configurations for the mixing of eigenstates.

from the quantum-mechanical modeling when the cavity is large enough, i.e., when it becomes truly semiclassical.

A complication arising from the periodic orbit theory in the present context is that it refers to the properties of an isolated billiard. In a more complete quantum description of magnetotransport the situation is more complex than just a density-of-states effect and a gradual depopulation of shells. In fact, the leads have an important role for the magnetoconductance, and the scattering states inside the billiard may actually be viewed as a linear combination of the eigenstates of the nominally isolated billiard.[11,12] The mixing occurs for states with energies in the close vicinity of E_F and the particular values of the mixing coefficients depend on the characteristics of the leads. For the triangular billiard, this is illustrated in Fig. 6(a) where the magnetoconductance $G(B)$ calculated quantum mechanically is shown for two different lead configurations, as indicated. Clearly, the overall behavior of the magnetoconductance is changed significantly when the lead at the side of the triangle is moved away from the symmetry axis. Classically, this behavior is expected because the trajectories that contribute to electron transport are entirely different when the point of injection is changed. Concerning the conductance fluctuations, however, one could expect less dramatic changes, because the scattering states inside the billiard, through which the electrons have to tunnel, are defined by the overall geometry of the billiard and should not be too different in the two cases. In fact, the Fourier transformations of the conductance data [Fig. 6(b)] show that the frequencies of the conductance fluctuations are almost exactly the same for both lead configurations, while the relative strength of the frequencies, i.e., the mixing of the billiard eigenstates, is different for different lead positions.

As the magnetic field is swept there is a rich variation of the linear combinations of states inside the billiard. If there exists any similarity with the classical picture it should be revealed in visualizations of the quantum-mechanical probability distributions of the density and the velocity. The following results are based on a particular scattering state in which the initial, incoming state is constructed as a symmetric linear combination of all incoming modes. Figure 7 shows the density and velocity distributions for the four cases $B/B_c=0$, 1, 2, and 3 (left and center column, respectively), together with plots of the classical trajectories of electrons injected into the billiard through the side opening (right column). In contrast to Fig. 3, the classical plots displayed in this figure contain the transmitted *and* the reflected trajectories, giving the complete classical density distribution. It appears that at zero field, the quantum-mechanical density and velocity distributions are actually almost more collimated than the corresponding collection of classical trajectories. There is a faint trace of scarring in the quantum-mechanical distribution that resembles a classical path connecting the two leads. This striking picture is, however, somewhat fortuitous because the spatial distributions are sensitive to small changes in Fermi energy, direction of current, etc. The same is true for the case $B/B_c=1$. In this case, one observes a spreading of the density distribution, which is consistent with the classical distribution in a rough way, but at the same time there are no signs of the kind of scarring one would expect intuitively from the skipping orbit indicated in Fig. 3(b).

The situation is changed at higher fields, where the electron wave function becomes increasingly localized. The halo observed for $B/B_c=2$ has obvious similarities with the classical case. For $B/B_c=3$, finally, skipping orbits emerge clearly in accordance with the classical case, and the quantum-mechanical and the classical density distributions are similar. To summarize the four cases, we find, in agreement with earlier findings,[11] that there is little resemblance between the quantum-mechanical and classical distributions at low fields. At higher fields, on the other hand, we find that the similarity becomes quite striking.

When the magnetic field is increased even further, edge states are fully developed. Figure 8 shows the spatial probability distributions for $B/B_c=5$ and for reversed field and current (voltage). One can clearly distinguish the collective excitation of several edge states extending over the entire edge region. The overall features are independent of direction of field and current, although fine details are dependent on these. In this sense the results appear to be in qualitative agreement with the classical simulations of different current directions in Fig. 3.

IV. SUMMARY

We have compared a classical and a quantum-mechanical approach to the analysis of the experimentally observed magnetoresistance of triangular electron billiards. In our discussions we have focused on the question to what extent (semi)classical dynamics can be used to model electron

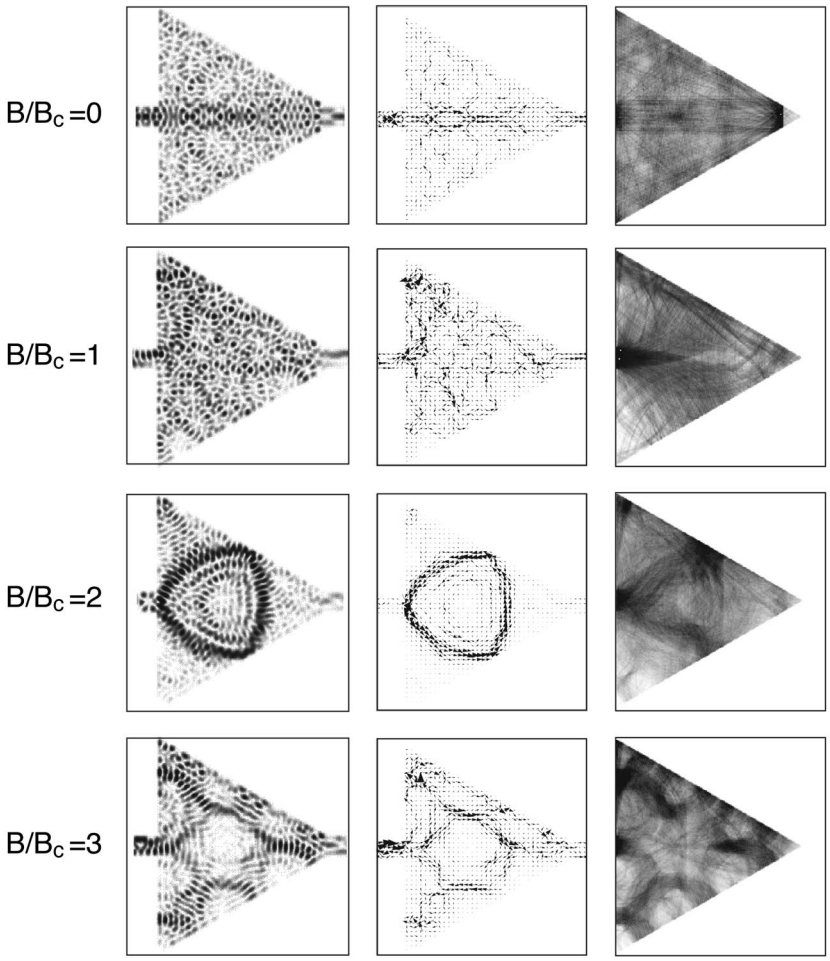

FIG. 7. Left-hand and center columns: Quantum-mechanical probability distributions for density and velocity, respectively, at different fields, obtained from Green's-function calculations. Broadening due to inelastic effects is not included in these graphs. The right-hand column shows the classical particle-density distributions for electrons injected through the side contact at the same magnetic fields.

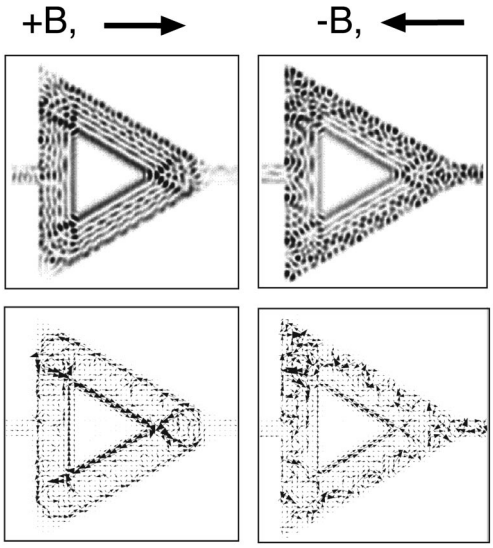

FIG. 8. Quantum-mechanical probability distributions for the particle density (top figures) and for the velocity (bottom figures) as obtained from Green's-function calculations with $B \simeq 5B_c$. The figures on the left are for reversed fields and currents as compared to the figures on the right. As in the previous figure, broadening due to inelastic scattering is not included.

transport, in comparison to a full quantum-mechanical treatment.

The classically simulated magnetoresistance was found to agree with the measured data in great detail, in particular at temperatures at which quantum interference effects are absent. The simple electron trajectories that were previously found to be of great importance for the magnetoresistance[8] were shown to be indeed abundant in plots of all possible electron trajectories at different magnetic fields. The frequency of quasiperiodic conductance fluctuations, experimentally observed at lower temperatures, were found to correspond to the area of the simplest reflected electron trajectory in the billiard. In conclusion, the (semi)classical model provides a consistent and complete understanding of the main features that were observed in the relatively large experimental sample.

The magnetoresistance calculated quantum mechanically reproduced the (classical) gross features of the experimental data as well as the existence of conductance fluctuations in the experimentally observed frequency range. These fluctuations can be understood as being due to changes in the transmission probability for electrons through the billiard, as the density of states is shifted diamagnetically. The density of states in the real billiard may be thought of as being the result of the mixing of eigenstates of the closed billiard, which in turn was shown to depend on the detailed position of the leads. Consequently, the results based on real samples can only within certain limits be related to the density of states of the ideal geometry.

A conceptual problem remaining concerns the detailed relation of classical electron trajectories and conductance fluctuations. While our experimental results and the semiclassical, periodic orbit theory suggest that the periodic orbits, distorted by the magnetic field, should be considered in order to explain the frequency of the fluctuations, the results from our quantum-mechanical calculations were not conclusive. It would be interesting to investigate the role of the size of the billiard in this context in more detail.

The interplay between the classical and the quantum-mechanical picture of electron dynamics was further studied by comparing classically and quantum-mechanically calculated particle-density distributions inside the billiard. At low magnetic fields, little resemblance between the two was found, which makes the success of the classical model of transport remarkable. At high fields, however, almost identical images of the particle density are obtained with the two techniques. It would be exciting to bridge the two approaches by adding a phase to the classical trajectories. This would also have the advantage that wave effects could be studied also in large samples, in which full quantum-mechanical calculations are numerically complicated and computationally as yet too demanding.

ACKNOWLEDGMENTS

The authors thank S. M. Reimann for valuable comments on the manuscript. The work was carried out within the Nanometer Structure Consortium in Sweden and was supported by the Swedish Engineering and Natural Science Research Councils, and by the Göran Gustafsson Foundation for Research in Natural Sciences and Medicine. We thank Claus B. Sørensen, the III-V NANOLAB, and CNAST for the MBE-grown structures. Support from the Royal Swedish Academy of Sciences (I.Z.) is gratefully acknowledged.

[1] C. W. J. Beenakker and H. van Houten, in *Solid State Physics*, edited by H. Ehrenreich and D. Turnbull (Academic, San Diego, 1991) Vol. 44, p. 1.

[2] R. A. Jalabert, H. U. Baranger, and A. D. Stone, Phys. Rev. Lett. **65**, 2442 (1990).

[3] C. M. Marcus, A. J. Rimberg, R. M. Westervelt, P. F. Hopkins, and A. C. Gossard, Phys. Rev. Lett. **69**, 506 (1992).

[4] C. Jung, Can. J. Phys. **58**, 719 (1980).

[5] M. V. Berry and M. Wilkinsson, Proc. R. Soc. London, Ser. A **392**, 15 (1984).

[6] M. Brack and R. K. Badhuri, *Semiclassical Physics* (Addison-Wesley, Reading, MA, 1997).

[7] The authors of Ref. 6 also point out that the analytic solutions for the eigenmodes were in fact available already in 1852 for the analogous problem of an elastic vibrating triangular membrane. Only numerical constants differ from the quantum case, see M. G. Lamé, *Leçons sur la Théorie Mathématique de L'élasticité des Corps Solides* (Bachelier, Paris, 1852).

[8] H. Linke, L. Christensson, P. Omling, and P. E. Lindelof, Phys. Rev. B **56**, 1440 (1997).

[9] P. A. Lee and T. V. Ramakrishnan, Rev. Mod. Phys. **57**, 287 (1985).

[10] K.-F. Berggren, Z.-L. Ji, and T. Lundberg, Phys. Rev. B **54**, 11 612 (1996).

[11] I. V. Zozoulenko, R. Schuster, K.-F. Berggren, and K. Ensslin, Phys. Rev. B **55**, R10 209 (1997).

[12] I. V. Zozoulenko and K.-F. Berggren, Phys. Rev. B **56**, 6931 (1997).

[13] M. Persson, J. Pettersson, B. von Sydow, P. E. Lindelof, A. Kristensen, and K. F. Berggren, Phys. Rev. B **52**, 8921 (1995).

[14] J. P. Bird, D. K. Ferry, R. Akis, Y. Ochiai, K. Ishibashi, Y. Aoyagi, and T. Sugano, Europhys. Lett. **35**, 529 (1996).

[15] S. M. Reimann, M. Persson, P. E. Lindelof, and M. Brack, Z. Phys. B **101**, 377 (1995).

[16] T. M. Fromhold, L. Eaves, F. W. Sheard, M. L. Leadbeater, T. J. Foster, and P. C. Main, Phys. Rev. Lett. **72**, 2608 (1994).

[17] L. Eaves, in *Proceedings of the 23rd International Conference on the Physics of Semiconductors*, edited by M. Scheffler and R. Zimmermann (World Scientific, Singapore, 1996), Vol. I, p. 43.

[18] I. V. Zozoulenko, F. A. Maaø, and E. H. Hauge, Phys. Rev. B **53**, 7975 (1996); **53**, 7987 (1996); F. A. Maaø, I. V. Zozoulenko, and E. H. Hauge, *ibid.* **50**, 17 320 (1994).

[19] C. M. Marcus, R. M. Westervelt, P. F. Hopkins, and A. C. Gossard, Phys. Rev. B **48**, 2460 (1993).

[20] R. M. Clarke, I. H. Chan, C. M. Marcus, C. I. Duruoz, J. S. Harris, K. Campman, and A. C. Gossard, Phys. Rev. B **52**, 2656 (1992).

[21] J. P. Bird, K. Ishibashi, D. K. Ferry, Y. Ochiai, Y. Aoyagi, and T. Sugano, Phys. Rev. B **51**, 18 037 (1995).

[22] H. Linke, J. P. Bird, J. Cooper, P. Omling, Y. Aoyagi, and T. Sugano, Phys. Rev. B **56**, 14 937 (1997).

[23] M. Brack, J. Blaschke, S. C. Creagh, A. G. Magner, P. Meier, and S. M. Reimann, Z. Phys. D **40**, 276 (1996).